ENVIRONMENTAL RESEARCH
LETTERS

PURPOSE-LED PUBLISHING™ Part of the ENVIRONMENTAL RESEARCH SERIES

LETTER • OPEN ACCESS

Compounding of 100-year coastal floods by rainfall in an urban environment

To cite this article: Shima Kasaei *et al* 2026 *Environ. Res. Lett.* **21** 024007

IOP Publishing Environ. Res. Lett. 21 (2026) 024007 https://doi.org/10.1088/1748-9326/ae2a55

ENVIRONMENTAL RESEARCH
LETTERS

OPEN ACCESS

RECEIVED
9 June 2025

REVISED
30 November 2025

ACCEPTED FOR PUBLICATION
9 December 2025

PUBLISHED
16 January 2026

LETTER

Compounding of 100-year coastal floods by rainfall in an urban environment

Shima Kasaei[1,*], **Philip M Orton**[1], **Thomas Wahl**[2], **David K Ralston**[3] and **John C Warner**[4]

[1] Stevens Institute of Technology, Hoboken, NJ 07030, United States of America
[2] University of Central Florida, Orlando, FL 32816, United States of America
[3] Woods Hole Oceanographic Institution, Woods Hole, MA 02543, United States of America
[4] United States Geologic Survey, Woods Hole Coastal & Marine Science Center, Woods Hole, MA 02543 United States of America
[*] Author to whom any correspondence should be addressed.

E-mail: skasaei@stevens.edu

Keywords: compound flooding, coastal flood hazard, flood risk assessment, extreme events, pluvial flooding, flood hazard maps

Supplementary material for this article is available online

Abstract

Coastal and pluvial flooding are both becoming more prevalent and severe due to climate change and urbanization in floodplains. The co-occurrence of these flood drivers is generally assumed to exacerbate the resulting flood impacts, a result referred to as compound flooding. However, few observational or modeling studies have investigated the circumstances under which this occurs. Here, we study the impacts of these combined flood drivers and evaluate the implicit hypothesis of official flood maps, which is that rainfall has a negligible impact on the flood depth and flooded area due to a 100 year coastal flood. A coastal system model, configured to capture coastal and pluvial flood drivers, is used. We evaluate the flooding for different urban landform types, including coastal landfill (human-made land), convergent areas (topographic depressions) and other urban terrain, within a model domain covering the Jamaica Bay watershed of New York City. A scenario-based strategy is adopted with a 100 year coastal flood as a control simulation, to which we add a set of realistic scenarios of rainfall data from historical tropical cyclones. We also apply a joint probability analysis framework with historical data to evaluate the probability of these compound coastal-pluvial scenarios. Results reveal cases where the pluvial driver compounds the coastal flood through expansion of the flood zone, with a 17% chance of rainfall increasing the flood area by 6%–38%, and a 5% chance of an increase of 61%–73%. It is rare that floods are significantly deepened but when deepening occurs, it is more common for the convergent zone than for the coastal landfill. These findings quantitatively assess the potential of the pluvial driver to exacerbate flooding, which may influence emergency management strategies such as evacuation plans, shelter arrangements, and related preparedness measures.

1. Introduction

Assessment of extreme event flooding typically emphasizes the 100 year event from a single driver, such as coastal storm tide, which forms the basis for Federal Emergency Management Agency (FEMA) flood maps (Rosenzweig *et al* 2018, Bates *et al* 2021), National Hurricane Center's SLOSH (Sea, Lake and Overland Surges from Hurricanes) flood hazard maps (Jelesnianski 1992, Zachry *et al* 2015), and real-time P-SURGE probabilistic flood forecast maps (Penny *et al* 2023). However, recent research has demonstrated that multiple flood drivers, such as combined pluvial (rain-driven) and coastal (surge-driven), can cause more severe flooding than individual flood drivers, highlighting the need to assess compound flood hazards (Orton *et al* 2012, Moftakhari *et al* 2017, Diermanse *et al* 2023).

Flooding driven by intense rainfall that overwhelms drainage systems, known as pluvial flooding, is becoming more frequent and severe due to climate change and urbanization (Rosenzweig *et al* 2018).

Studies show that pluvial flooding accounts for 74% of tropical cyclone (TC) and 60% of non-TC flood insurance claims in the U.S. (Tonn and Czajkowski 2022). Pluvial flooding is particularly problematic in urbanized areas, where impervious surfaces and inadequate drainage intensify flood impacts (Pallathadka *et al* 2022, Lin *et al* 2023). Key factors influencing urban pluvial flooding include topography, rainfall intensity, and the extent of impervious surfaces, which vary significantly (Qi *et al* 2020). In coastal urban settings, upland areas are critical for evacuation roads from coastal flood zones, which motivates the need to consider compound flooding that incorporates both coastal and pluvial components (Kurum *et al* 2022).

Statistical methods have been widely used to estimate the likelihood of compound extreme flood events (Thompson and Frazier 2014, Xu *et al* 2018, Zellou and Rahali 2019, Jane *et al* 2022, Kim *et al* 2023). Recent advances in compound flood modeling have introduced hybrid frameworks that combine statistical analysis with dynamical simulations to address multi-driver flood hazards (Wang *et al* 2024), offering new pathways for evaluating return periods and joint risks beyond conventional univariate metrics. However, there is still no consensus on standardized methods for compound flood mapping, and existing approaches often involve subjective assumptions and large scenario sets (Jane *et al* 2022). Recent work demonstrated large discrepancies between 100 year joint probability events for drivers (rainfall and storm surge) and 100 year flood events (Santamaria-Aguilar *et al* 2025).

This study presents a targeted, scenario-based approach to evaluate pluvial compounding of coastal extreme flooding across three coastal-urban landforms. Using a hydrodynamic model integrating both drivers, we hold a 100 year coastal baseline fixed and superimpose realistic tropical-cyclone rainfalls (observed and scaled, with varied intensities, spatial patterns, and timing) to isolate rainfall's marginal contribution to flood extent and depth. In doing so, we directly test the assumption underlying regulatory coastal flood maps that rainfall has minimal influence on flood extent and depth during a 100 year coastal event, and we evaluate whether current flood maps adequately reflect compound flood hazards in low-lying developed areas. This mechanistic approach complements existing statistical methods by directly testing compound driver in urban environments.

2. Methods

2.1. Study site

The Jamaica Bay watershed of New York (figure 1(a)) is home to over 2.8 million people (NYC-DEP 2018) and is highly vulnerable to both coastal and pluvial flooding. Approximately 7380 residential buildings were damaged or destroyed in neighborhoods around Jamaica Bay due to coastal flooding from Hurricane Sandy in 2012 (NYC 2013), the region's largest storm tide in over 300 years (Orton *et al* 2016). During Hurricane Ida in 2021, NYC's most extreme rain event in recorded history (NPCC4 2024), an estimated 4621 buildings were exposed to pluvial flood water deeper than 0.3 m (Kasaei *et al* 2025). Jamaica Bay has undergone significant man-made changes, including dredging, landfilling, and urbanization, which have altered its geomorphology and increased flood risks (Orton *et al* 2020). The watershed's diverse landscape, including residential areas, estuarine ecosystems (figure 1(b)), and critical urban infrastructure, necessitates a comprehensive approach to flood risk management and makes it an ideal candidate for a study site (Smith *et al* 2018).

2.2. Modeling

The Coupled Ocean Atmosphere Wave and Sediment Transport (COAWST) framework integrates ocean, atmosphere, surface wind waves, sediment transport to simulate coastal system interactions (Warner *et al* 2010). We use COAWSTv3.8 for Jamaica Bay that has previously been developed and evaluated (Kasaei *et al* 2025). Importantly, the model incorporates rainfall volumetric effects and infiltration/stormwater drain rates to assess rainfall impacts on coastal flood hazard maps.

Boundary conditions are derived from a large-scale coastal model (Hegermiller *et al* 2022). The Jamaica Bay watershed model contains 818 × 734 cells at an average horizontal resolution of 46 × 51 m with eight vertical sigma layers. Model bathymetry is obtained from composite bare Earth digital elevation model integrating National Park Service datasets (Flood 2011), NOAA NCEI 1/9th arcsec resolution DEM (Digital Elevation Model) (Cires 2014a) and 1/3rd arcsec resolution bathymetric data (Cires 2014b). Bottom friction uses spatially variable roughness parameters with quadratic coefficients determined from Coastal Change Analysis Program (C-CAP) land cover classifications (National Oceanic and Atmospheric Administration 2016). Manning numbers corresponding to C-CAP values (0.02–0.13) (Mattocks and Forbes 2008) are used to derive bottom roughness (Z_0) and subsequently the quadratic bottom roughness coefficient for model input. The model operates with 2.5 s baroclinic timestep and 20 barotropic sub-steps, using 5 cm critical depth threshold for wetting/drying (Warner *et al* 2013). Meteorological forcing comes from the North American Mesoscale Forecast System (NAM) 12 km analysis dataset (EM Center 2017).

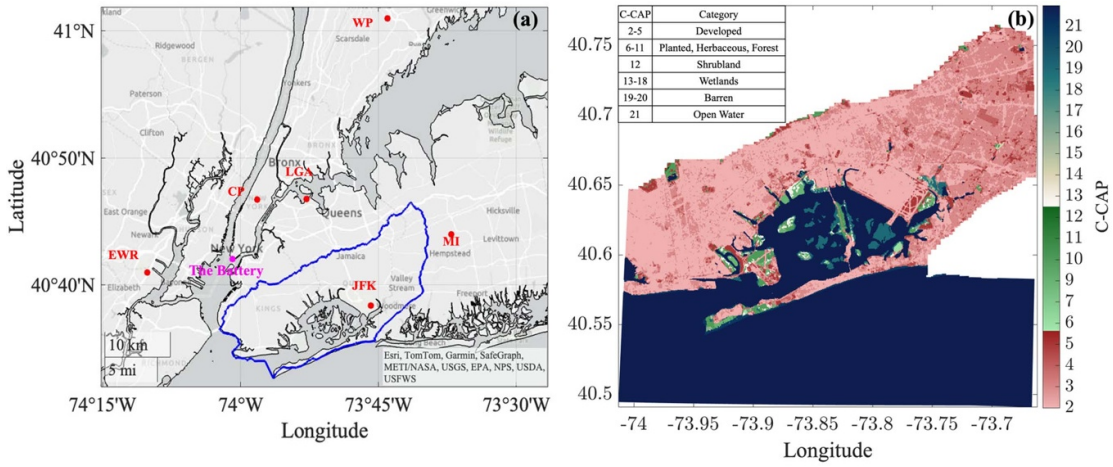

Figure 1. (a) Jamaica Bay watershed location (blue line) shown with rainfall gauges (red circles) at White Plains (WP), Mineola (MI), LaGuardia Airport (LGA), John F. Kennedy International Airport (JFK), Central Park (CP), and Newark Liberty International Airport (EWR); and The Battery station tide gauge (magenta dot), (b) Coastal Change Analysis Program (C-CAP) values and the land-cover categories in the Jamaica Bay watershed.

2.3. Coastal 100 year flood and historical tropical rain events

For the purposes of this study, we simulate Hurricane Sandy as a sample 100 year coastal flood. Hurricane Sandy in October 2012 caused extensive flooding and significant damage across the New Jersey–New York and broader coastal regions, including Jamaica Bay and surrounding neighborhoods (Wang *et al* 2014). The storm's impact was influenced by factors such as the arrival of peak surge at high tide (Georgas *et al* 2014) and urban coastal vulnerability (Hopper and Meixler 2016). While studies estimate Sandy's peak water level return period at ∼100 (Lopeman *et al* 2015) to ∼850 years (Lin *et al* 2012), it closely matches the official FEMA (2014) 100 year storm tide for both New York Harbor (NYH) and Jamaica Bay. We simulate the response from Sandy and compare the inundation zones with FEMA 100 year coastal flood hazard zones to assess its validity as a sample 100 year coastal flood. The Sandy simulation for the nested model is initiated with a model time of 25 October 2012, 00:00 UTC and run for 5.5 d to 30 October 2012, 12:00 UTC. The NAM model provides wind speed, atmospheric pressure, relative humidity, air temperature, and short and long wave radiation data on a 12 km spatial grid and 3-hour temporal resolution. A larger scale model provides boundary conditions including free surface elevation, depth-averaged and three-dimensional velocity components (u and v), temperature, and salinity fields for domain boundaries with ∼0.7 km spatial resolution and hourly temporal resolution.

To include pluvial effects, realistic rainfall scenarios are developed based on historical hurricane events to capture how precipitation intensity, spatial distribution, and timing affect compound flooding. Since a hurricane storm surge event is by far a more likely cause of a 100 year storm tide at NYH than extratropical cyclones (Orton *et al* 2016, Marsooli *et al* 2019), we focus on hurricane surge-associated rainfall patterns. Hurricanes Irene (2011), Gloria (1985), Donna (1960), and Ida (2021), are selected based on their spatial diversity in rainfall patterns and wide range of rainfall intensities (8.6–25.9 mm hr^{-1} peak rates) (figure 2). These storms capture contrasting spatial distributions with Irene and Ida both exhibiting heavier rainfall toward the western portion of the domain, Donna had higher totals in the east, and Gloria displaying more uniform precipitation across the entire area. Each storm's rainfall footprint is reconstructed using available observational data. Observations from six NOAA rain gauge stations surrounding the study region (figure 1(a)) are interpolated over the model domain with an inverse-distance-squared-weighting method. This approach places greater emphasis on the gauges nearest each interpolation point, thereby preserving realistic spatial gradients in rainfall intensity.

The hyetographs representing spatial averages over the model domain (figure 3) preserve the observed magnitude, average peak and the temporal sequencing of rainfall relative to the storm surge. Storm surge at The Battery gauge (figure 1(a)) is computed as the residual water level after removing the annual mean sea level and astronomical tides predicted using harmonic analysis (T_TIDE) (Pawlowicz *et al* 2002), with removal of seasonal variations using a 15 day running average of daily climatology. Retaining the real-world time lags between peak rainfall and peak storm surge ensures that the baseline scenarios reflect historic conditions rather than purely synthetic events. In all these cases, the peak of the surge occurs after the rainfall peak. The temporal lags between peak rainfall and peak surge

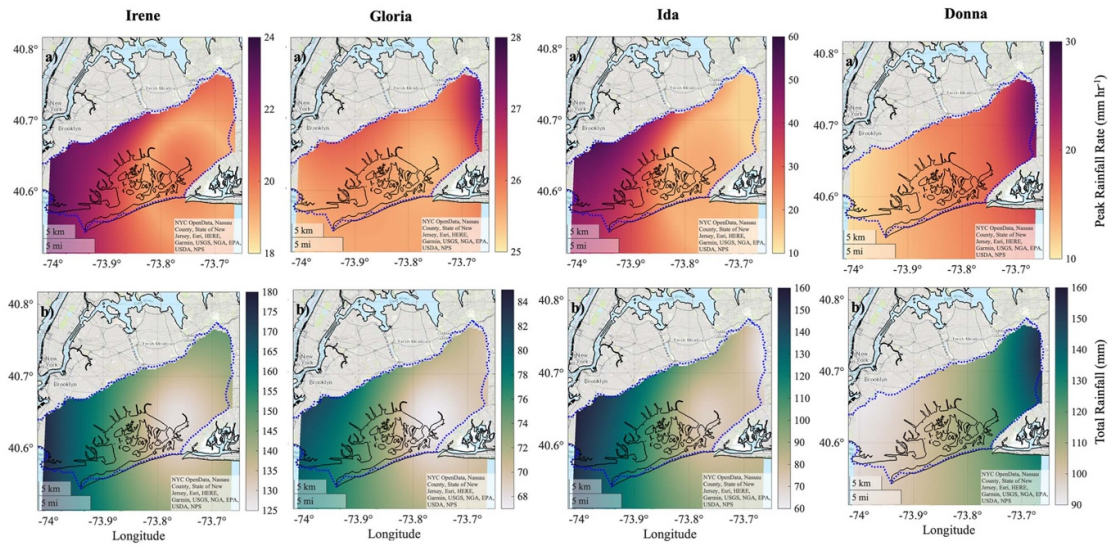

Figure 2. Maps of (top) Storm-maximum rainfall rate (mm hr^{-1}) and (bottom) rainfall total accumulation (mm), for Hurricanes Irene, Gloria, Ida, and Donna.

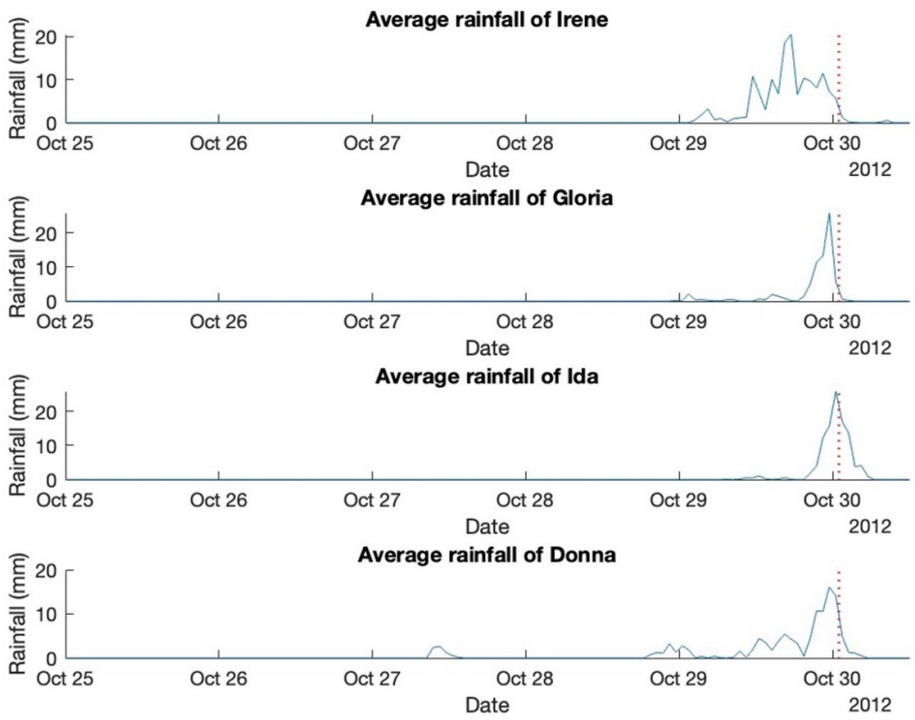

Figure 3. Spatial average of rainfall scenarios over the land, red dots show the Sandy peak surge on 30 October 2012, 01:00 UTC/GMT.

for Irene, Gloria, Ida, and Donna are 7.5 h, 1.5 h, 0.5 h, and 1.5 h, respectively.

2.4. Synthetic scenarios spanning intensity, spatial variation and timing lag

To evaluate sensitivity to storm intensity, several scenarios are defined based on Hurricane Ida's peak spatially averaged rainfall intensity: full-intensity (equal to Ida's maximum, SC1), two-thirds (2/3 × Ida's maximum, SC2/3rd), and one-third intensity (1/3 × Ida's maximum, SC1/3rd). These scaled intensities are applied proportionally to each storm's rainfall pattern, preserving spatial distributions while systematically varying overall rainfall intensity. These intensity levels (8.6, 17.2, and 25.9 mm hr^{-1}) correspond to the 56th, 83rd, and 95th percentiles of rainfall observed during historically top-ranked TC surge events (see section 2.6), ensuring scenarios reflect realistic compound event probabilities. This approach enables systematic evaluation of compound flooding across the

Table 1. Summary of flood modeling scenarios. All scenarios include Sandy storm surge and astronomical tides except rainfall-only. MOM = maximum of maximum across all four storm patterns.

Scenario	Description	Rainfall intensity	Storm patterns	Ocean forcing
Control	Hurricane Sandy coastal flood	None	N/A	Sandy surge + tide
+Ida	Sandy + Ida rainfall	Ida's observed	Ida spatial pattern	Sandy surge + tide
+Irene	Sandy + Irene rainfall	Irene's observed	Irene spatial pattern	Sandy surge + tide
+Donna	Sandy + Donna rainfall	Donna's observed	Donna spatial pattern	Sandy surge + tide
+Gloria	Sandy + Gloria rainfall	Gloria's observed	Gloria spatial pattern	Sandy surge + tide
SC1	Scaled to full intensity	100% of Ida's peak	Each of 4 patterns individually	Sandy surge + tide
SC2/3	Scaled to 2/3 intensity	67% of Ida's peak	Each of 4 patterns individually	Sandy surge + tide
SC1/3	Scaled to 1/3 intensity	33% of Ida's peak	Each of 4 patterns individually	Sandy surge + tide
MOM SC1	MOM at full intensity	100% of Ida's peak	Cell-wise maximum across all 4	Sandy surge + tide
MOM SC2/3	MOM at 2/3 intensity	67% of Ida's peak	Cell-wise maximum across all 4	Sandy surge + tide
90 min lag	Temporal shift scenarios	Variable	Each of 4 patterns individually	Sandy surge + tide

observed range of rainfall intensities during extreme surge events. To capture the maximum potential compound flooding impact, we use model results to generate maximum of maximum (MOM) maps representing cell-wise maximum flood depth across the four historical rainfall patterns (Ida, Irene, Donna, and Gloria) for each of the three intensity scenarios, creating an envelope of worst-case flooding conditions. This approach identifies areas most vulnerable to compound flooding for a range of storm patterns and provides flood hazard information for emergency management planning (Jelesnianski 1992, Abdalla and Niall 2009, Zachry *et al* 2015). Additionally, we simulate a worst-case temporal scenario set where rainfall peaks 90 min before the surge crest, reflecting the watershed's time of concentration (calculations are shown in supplementary material). This shifted alignment maximizes the overlap in flooding between pluvial and coastal drivers. (table 1).

2.5. Investigating the role of urban landforms

To assess how topography might moderate or exacerbate flooding and generalize our findings for common coastal-urban landforms or geomorphic settings, the influence of land slope on pluvial–coastal compounding is also examined. The Jamaica Bay watershed encompasses three principal landforms: comparatively flat, coastal landfill (median slope of 14.1°), adjacent convergent depressional zones (median slope of 15.6°), other urbanized terrain (median slope of 21°). Coastal landfill areas consist of artificially created land formed by filling in coastal wetlands and waterways with sediment or other materials (Zhang and Orton 2022). Convergent depressional zones are low-lying areas where surface water naturally accumulates due to surrounding topography. These areas are identified using geomorphometric terrain classification combining pit, channel, and ridge classes where topographic convergence index exceeded the mean. Convergent zones often occur in the coastal-urban environment due to landfill and subsequent settling or compaction (Shirzaei and Bürgmann 2018). Examining each setting in turn allows for a rigorous assessment of how land surface gradient modulates the compound interplay between pluvial and coastal flooding.

2.6. Probabilistic context

We assess joint occurrence probabilities using historical hourly rain and surge data (Sadegh *et al* 2018). As noted in section 2.3, a TC storm surge event is by far the most likely cause of a 100 year storm tide at NYH, so our assessment of joint occurrence of rain is conditional on there being a top-ranked surge event (top 750 events over the 75 year analysis period). We first selected the top 750 surge events over the 75 year analysis period, then filtered this subset to retain only TC events, yielding approximately 25 TC-driven events for analysis. To account for watershed response time, we incorporate a 90 min lag between peak rainfall and surge when generating rain-surge pairs. This temporal adjustment reflects the concentration time in an idealized simulation of pluvial flooding on the watershed, allowing for more realistic representation of compound flooding dynamics. We consider TCs events within a 250 km radius of the area, which is a typical search radius used in studies of storm surge (e.g. Lin *et al* (2010)) and for which there is also often rainfall at NYH. The multi-hazard scenario analysis toolbox (MhAST; Sadegh *et al* (2018)) provides tools for assessing dependency and joint probability. Dependency of rain and surge is evaluated using Kendall rank, Pearson product-moment, and Spearman rank correlations. Joint probabilities are calculated using empirical rainfall percentiles and theoretical distribution fitting for return period estimation.

2.7. Limitations

Several limitations of our modeling approach should be acknowledged. Our use of Hurricane Sandy as a representative 100 year coastal flood, while validated against FEMA maps, may not capture the full range of meteorological conditions that could produce similar

return period events. Moreover, the use of Sandy as a nominal 100 year extreme coastal flood has uncertainty (100–850 years) (Lin *et al* 2012, Lopeman *et al* 2015). While Sandy was an unusual storm, its storm tide duration of 4.5 h above a severe flood threshold of 2.0 m is very typical in comparison to the median duration of 3.82 h (standard deviation of 1.84 h) among a broader set of 22 synthetic ∼100 year storms from a recent flood hazard assessment (Orton *et al* 2016).

The model uses a constant drainage rate that does not explicitly respond to surge-induced outfall failure. To examine the potential bias this introduces, we conduct a sensitivity analysis in which drainage is disabled in the coastal flood zone when the water level exceeds the minor flood threshold (indicating flooding of the lowest-lying streets). The model's 46 × 51 m grid resolution also limits the representation of fine-scale topography and surface roughness variations, and our use of only four historical rainfall patterns and a small set of different lag times to develop compound flood scenarios may not fully capture the range of possible precipitation distributions during extreme coastal events.

3. Results

3.1. 100 year coastal flood

First, Hurricane Sandy is simulated as a coastal flood with no rain forcing (figure 4). Our Sandy inundation covers 133 km^2 (27% of urban area) compared to FEMA's 100 year flood zone of 103 km^2 (21% of urban area). The additional flooded area occurs primarily inland behind JFK airport, reflecting dynamic coastal processes captured by the hydrodynamic model. This agreement supports using Sandy as representative of a FEMA 100 year flood.

3.2. Effect of rainfall on the 100-year coastal flood

Rainfall is then added to examine compound flooding impacts. Simulations using historical rainfall events reveal the substantial influence of precipitation on flooding extent. When rainfall is added to the coastal flood baseline (control case), the total flooded area increases considerably across all combined scenarios. For example, the flooded area (depth > 0.05 m) expands from 98 km^2 in the coastal case to 158 km^2, 125 km^2, 145 km^2, and 145 km^2 with the observed rainfall from Ida, Donna, Irene and Gloria, respectively. Scaling the rainfall patterns from Donna and Irene to Ida's rainfall intensity increases flooded areas from 125 km^2 to 170 km^2 and from 145 km^2 to 166 km^2, respectively. The MOM map (explained in section 2.4) shows the flooded area reaches 194 km^2 under a composite scenario (SC1) representing the maximum depth across all rainfall events scaled to Hurricane Ida's intensity (figure 5(a)).

Similarly, the MOM results show that deep flooding areas (depth > 0.3 m) increase with rainfall intensity (figure 5). Compared to 86 km^2 in the coastal case, the control case with Ida, Donna, Irene, and Gloria results in 98 km^2, 89 km^2, 90 km^2, and 90 km^2 of deep-to-severe flooding, respectively (figure 5(a)). When Donna and Irene are scaled to the 2/3rd intensity of Hurricane Ida, the deeply flooded area increases to 103 km^2 and 99 km^2, respectively, while Gloria's scaled rainfall produces the same deeply flooded area. This confirms that adding rainfall consistently increases the flood extent, especially in inland areas. Deeply flooded area reaches to 112 km^2 (23% of the watershed) for MOM SC1, and 94 km^2 (19.4% of the watershed) for MOM SC2/3rd.

In terms of depth distribution (figure 5(b)), MOM SC1 scenarios produce the largest percentage of severely flooded areas (>0.9 m), followed by the control case with Ida and the MOM 2/3rd. The coastal scenario shows almost no severe flooding and is dominated by moderate depths, again illustrating the critical contribution of rainfall to urban flood severity.

To assess how flood impacts vary with rainfall intensity, we developed synthetic rainfall scenarios scaled to the peak intensity of Hurricane Ida (see Methods for details). The spatial pattern of flooding for the MOM SC1 (figure 6(a)) demonstrates widespread inundation, especially across densely urbanized zones. The rainfall-only contribution (figure 6(b)) shows significant inland flooding after removing the coastal flood influence, reinforcing the dominant role of rainfall in driving urban flood risk.

Temporal sensitivity analysis shows that shifting rainfall timing to a 90-minute lag results in mild increase in significantly deeper flooded areas only for Irene (from 0.40 km^2 to 0.67 km^2), which has the longest original lag (7.5 h). Other storms with shorter original lags (Ida: 30 min; Donna and Gloria: 90 min each) remain largely unchanged, suggesting their timing is already near optimal. These findings indicate that although temporal phasing affects flooding, rainfall intensity remains the dominant factor at the watershed scale.

3.3. Landscape effects on compounding

Topography analysis revealed distinct land slope influences compound flooding. Coastal landfill areas (37.92 km^2) and convergent areas (5.3 km^2) are mutually exclusive, but both occur within the coastal flood zone (122.6 km^2), plus other urban terrain. The urban area above 0 meters (484.8 km^2), which is predominantly urban terrain, shows minimal compounding effects for flood depth. More than 40% of coastal flood zone experiences additional flood depth when rainfall is added, with significantly deeper flooding (depth compounding >5 cm) affecting just 0.002–1.4 km^2 (0.002%–1.2% of the area) even in extreme scenarios. Urban terrain experienced additional flooding extent from rainfall.

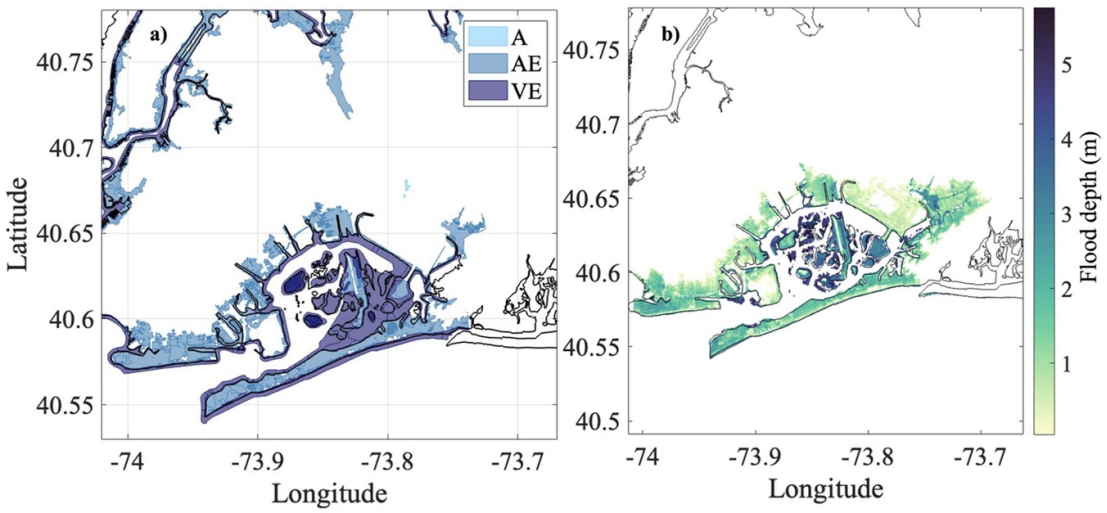

Figure 4. (a) Flood hazard zone map by FEMA, where the zones A (1% annual chance floodplain), AE (1% annual chance floodplain with base flood elevations) and VE (1% annual chance coastal high hazard area) combined to form the 100 year flood zone, (b) maximum flood depth for the Sandy simulation on the Jamaica Bay watershed.

Coastal landfill areas (figure 7), demonstrate widespread shallow depth compounding. Although 40%–93% of these areas experience additional flood depth when rainfall is added, the area with significant depth increases (>5 cm) is small, affecting up to 1.3% of the area and maximum depth increase of 0.03% under extreme scenarios. This suggests that while coastal landfill is vulnerable to depth compounding, the depth increases are predominantly minor.

Convergent areas demonstrate heightened vulnerability to depth compounding. Up to 91% of these areas experience deeper flooding, with 2%–42% experiencing additional depths >1 cm and 0.04%–9% experiencing >5 cm increases. In extreme scenarios, maximum depth increases by 0.72%. A notable example is 'The Hole', a low-lying neighborhood in Jamaica Bay (figure 7), that exemplifies this vulnerability with up to 59% of its area experiencing significant depth increases. These depressions create natural basins where coastal surge and rainfall accumulate, showing substantially greater vulnerability than surrounding terrain.

Sensitivity analyses in which drainage capacity is disabled during coastal surge highlight the influence of surge-compromised drainage on deeper inundation. In these tests, the fraction of coastal flood zone with >5 cm depth increases rises from 1.17% to 12%. Landfill areas show a similar amplification, with significant depth increase (>5 cm) rising from 1.3% to 9%, with additional 0.02% of the maximum depth increase. Convergent areas also exhibit greater sensitivity, with up to 33% of their extent exceeding 5 cm depth increases and maximum depth increases more than doubling to 2.2%. These results demonstrate that while surge-driven drainage blockage intensifies flooding locally, the broader system-level flooding patterns remain consistent.

3.4. Probabilistic context

Examining rain-surge dependence, we apply multiple correlation measures to assess the strength of association between these variables. Kendall's rank correlation coefficient is 0.111 ($p = 0.454$), with similarly weak correlations found using Spearman's rank-order correlation (0.131, $p = 0.533$) and Pearson product-moment correlation (0.171, $p = 0.415$). These results are consistent with a previous study of this area (Chen *et al* 2025) and indicate weak, statistically non-significant dependence. While TCs can physically couple rainfall and surge processes, the observed correlations in our dataset suggest the impact of this coupling is relatively weak. The diverse temporal lags between peak rainfall and surge in our historical storms (30 min to 7.5 h) further support treating these processes as relatively independent. We acknowledge this represents a simplification, but it provides a reasonable approximation given the statistical evidence and limited number of historical events and is consistent with other compound flood studies. As the correlation is not statistically significant, we treat rainfall and surge as independent variables in our subsequent joint probability analyses. Below, we present two sets of results: (1) the probability of exceeding each rain intensity, given a top-ranked TC surge event is occurring, (2) the computed joint return periods of such events.

A scatterplot and cumulative density function (CDF) of rain for the top-ranked historical TC surge events is shown in figure 8. Rainfall intensities of 25.9, 17.2, and 8.6 mm hr^{-1} (SC1, SC 2/3rd, and SC 1/3rd in section 2.4) correspond to the 95th, 83rd, and 56th percentiles, with exceedance probabilities of 5%, 17%, and 44%, respectively. Based on figure 5(a), deeply flooded area increases range from 0%–5%

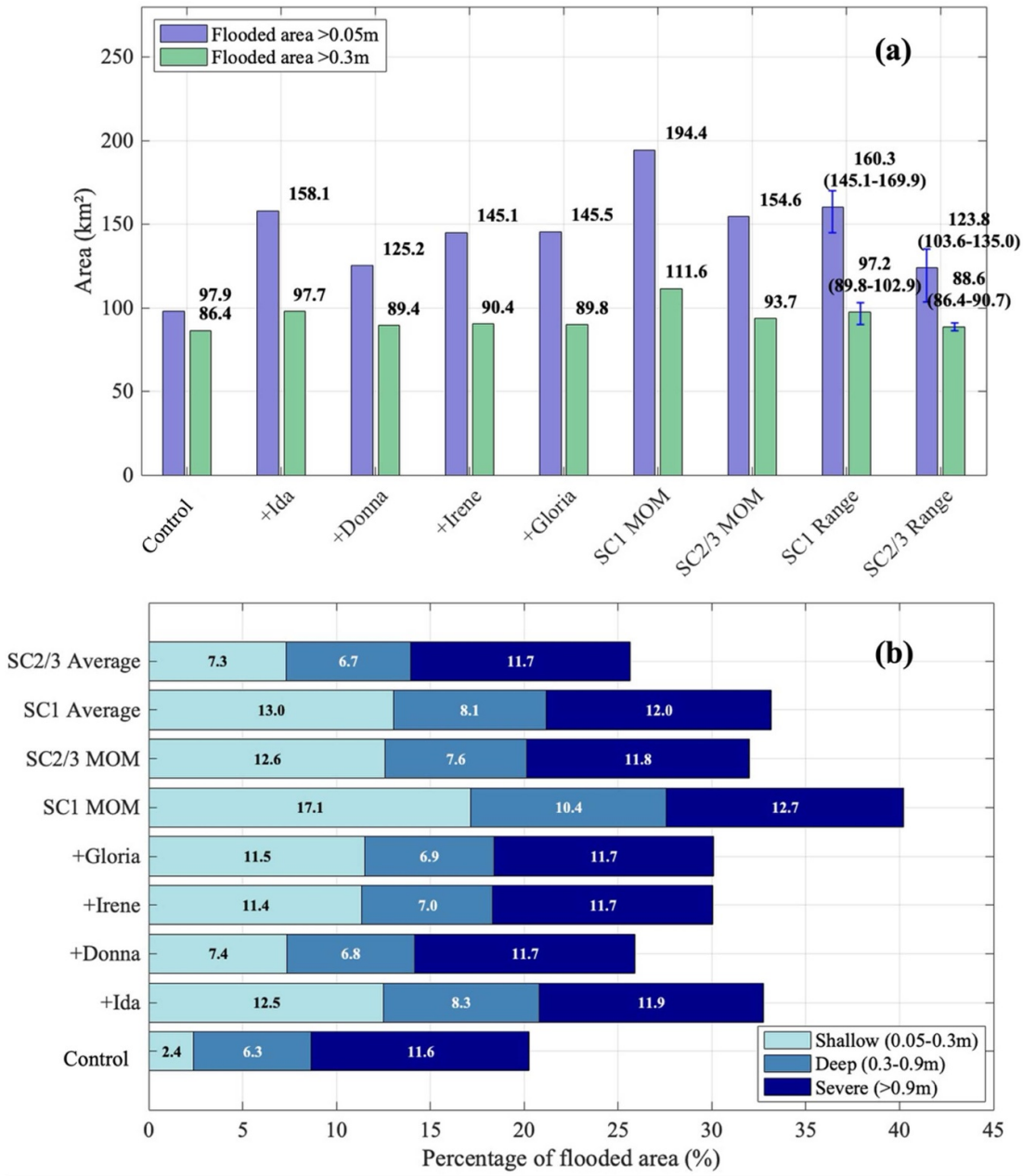

Figure 5. Flood extent and depth distribution across different rainfall scenarios. (a) Total flooded area with water depths >0.05 m and >0.3 m. Error bars represent the range of values across different storm patterns within each scenario. Numbers in parentheses show minimum and maximum flooded areas across the scaled intensity scenarios. (b) Percentage of flooded area by depth category (shallow, deep, severe). SC1 and SC2/3 refer to different scaled rainfall scenarios. MOM (maximum of maximum) represents the envelope of worst-case flooding conditions derived from cell-wise maximum flood depths across all four historical storm patterns. The hurricane names (+Ida, +Irene, +Donna, and +Gloria) indicate rainfall scenarios. 'Range' shows minimum and maximum values across scaled scenarios, while 'Average' shows mean values.

for SC2/3 scenarios and 4%–19% for SC1 scenarios compared to coastal flooding alone (86 km^2). We conclude that during a 100 year coastal flood, there is a 17% chance of rainfall causing an increase in deeply flooded areas by 0%–5% (8% in the MOM case); and a 5% chance of an increase by 4%–19% (29% in the MOM case).

The joint return period for each simulated scenario equals the inverse of the product of the individual exceedance probabilities. Rainfall for top-ranked surge events is best represented by an exponential marginal distribution, while surge heights fit a Generalized Pareto distribution; both marginals satisfy the goodness of fit test. Sandy's storm surge return period, estimated using maximum likelihood estimation with the Generalized Pareto distribution, produces an exceedance probability of approximately 1.4% for the fixed surge height (2.58 m) applied in all scenarios. Results are shown in table 2.

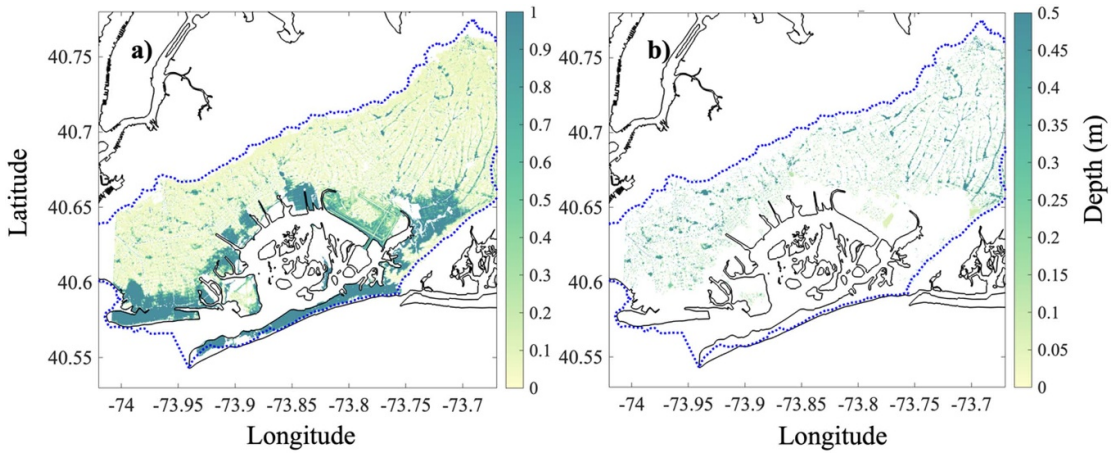

Figure 6. Spatial distribution of flood depths (in meters) across the study area. Panel (a) shows the total flood depth during the compound event, while panel (b) shows the rainfall-induced flooding component (panel a minus coastal-only baseline). Note the reduced flooding near the bay in panel (b) and persistent inland flooding patterns. Flood depths are shown for MOM SC1 (see Methods for scaling details).

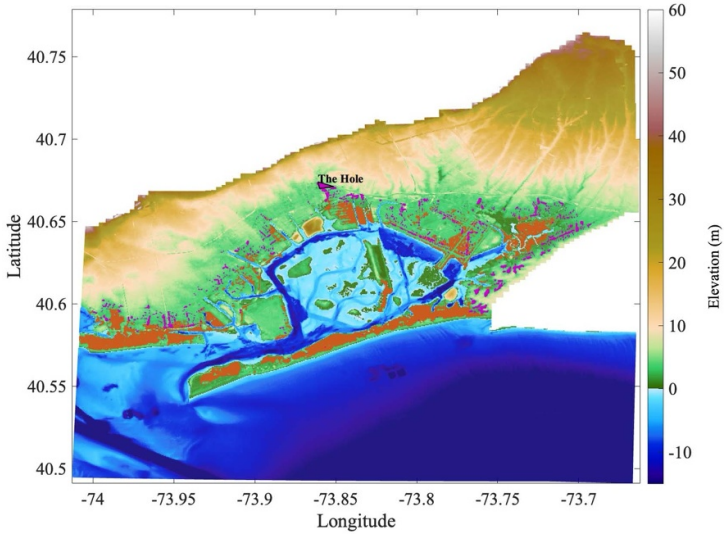

Figure 7. Topographic influence on compound flooding. Digital elevation model showing the topography of the study area with elevation (in meters) indicated by the color bar. The amber shading shows the coastal landfill neighborhood, the magenta shading shows the convergent areas, and 'The Hole' neighborhood is marked.

4. Discussion

This study's results challenge a critical implicit assumption in current coastal flood hazard and forecast maps: that rainfall has minimal influence on flood extent and depth during extreme coastal events. This finding is relevant to FEMA maps, NHC SLOSH maps, and NHC P-SURGE flood forecast maps. Our findings reveal that when rainfall is incorporated into a 100 year coastal flood scenario, there is a moderate probability (17%) that the extent of flooding will increase substantially (up to 38% expansion in total flooded area or 5% expansion of deeply flooded area) beyond what is captured in flood maps created with only the coastal flood drivers. Our landform-specific results suggest differentiated planning approaches: coastal landfill areas could benefit from improved drainage and barriers to manage lateral expansion, while convergent areas may need enhanced pumping and storage systems to address depth increases. The spatial mapping of increased flood area provides valuable information for emergency management, including strategic placement of evacuation routes and shelters based on landform-specific risk patterns.

These results demonstrate that although FEMA incorporates storm surge hazards using outputs from sophisticated models, it could be beneficial for their methods to account for rain. Incorporating rainfall expands the flood area, creating a substantial additional flood risk beyond designated flood zones. This aligns with recent research on compound flood

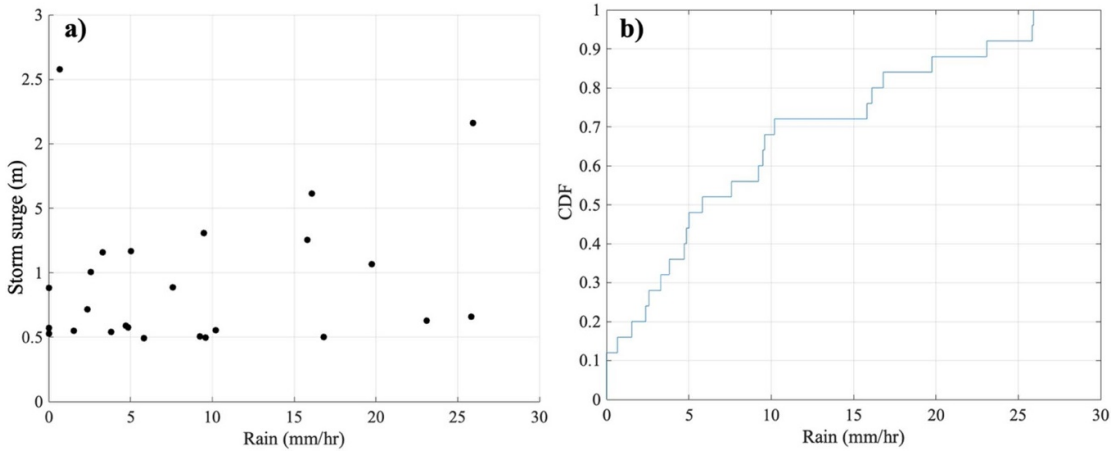

Figure 8. (a) Scatter plot showing pairs of rainfall intensity during top-ranked surge events (mm hr^{-1}) and storm surge (m). (b) Cumulative distribution function (CDF) of rainfall intensity for the selected events, showing the probability distribution of rainfall rates during surge-rainfall events.

Table 2. Compound exceedance probabilities and return periods for simulated tropical cyclone events.

Peak rain rate (mm hr^{-1})	$P(R \geqslant r)$	$P(S \geqslant 2.58$ m)	P_{joint}	Return period
25.85	0.05	0.014	0.0007	1428
17.24	0.17	0.014	0.0024	416
8.6	0.44	0.014	0.0062	160

drivers in urbanized coastal areas (Lewis *et al* 2024, Ali *et al* 2025, Amini *et al* 2025), suggesting current risk communication tools may provide a false sense of security to residents outside designated flood zones, particularly in urban areas where rainfall-driven flooding can be significant.

This study offers a rare glimpse into how the pluvial flood driver modifies a coastal (surge-driven) flood. It increases deeply flooded area (depth $>$ 0.3 m) by 4%–30%, depending on the scenario (30% in the MOM SC1, representing the worst-case envelope across all storm patterns). However, it has a relatively minor impact on flood depth; of the areas already flooded by the coastal flood in this urban environment, well below 1% show significantly increased flood depth ($>$5 cm) due to the compounding pluvial driver. The temporal analysis reveals that the phasing between rainfall and storm surge peaks can influence flood outcomes. Our finding that aligning rainfall with the watershed's time of concentration (90 min lag before surge peak) produced a measurable but limited increase in flooding extent for one of the storms (Irene) highlights that while temporal dynamics play a role in compound event assessment, their influence is secondary to rainfall intensity. This suggests that rainfall timing, though relevant, is not a critical factor in compound flood risk for this watershed.

Distinct flooding responses observed across flat coastal landfill, convergent areas, and other urban terrain demonstrate that topographic features influence vulnerability to compound flooding. The extreme vulnerability of convergent areas like 'The Hole' neighborhood highlights the need for neighborhood-scale assessment of compound flood risks. In this neighborhood, over half the area had deeper flooding in extreme scenarios and localized depth increases by 9%, highlighting how basins concentrate both storm surge and rainfall runoff. Coastal landfills present a more complex pattern: while most of these areas experienced some depth compounding when rainfall was added, significant depth increases ($>$5 cm) remained limited to only less than 2% of the area. In contrast, other urbanized terrain areas had minimal increases in flood depth but some increase in flooding extent.

In flood hazard assessment practice, the spatial compounding in the coastal landfill and other urbanized terrain regions can likely be reasonably represented by separate simulations of pluvial and coastal floods. However, the depth compounding effects in convergent regions require integrated compound flood modeling to capture the true flood hazard. This is because a non-linear relationship exists between coastal and pluvial processes, requiring consideration of momentum exchange between these flood drivers (Santiago-Collazo *et al* 2019).

The probabilistic analysis provides important context for risk management applications. These return periods provide a quantitative basis for

ranking the simulated compound floods and assessing their relevance to design and risk management thresholds in the study area. However, the simulated scenarios only examined the influence of rainfall on a 100 year return period coastal flood. A wider range of rain-surge joint extremes is possible that could cause compound flooding. With climate change likely to increase the frequency of Sandy- and Ida-like events (Lin *et al* 2016, Rosenzweig *et al* 2024), return periods presented here could shrink. Emerging evidence from other estuaries such as San Francisco Bay (Wang *et al* 2025) similarly shows that neglecting compound interactions underestimates risk, underscoring the value of integrated modeling for climate-resilient planning.

5. Summary and conclusions

Building upon previous pioneering research in compound flooding (e.g. Svensson and Jones 2004, Orton *et al* 2012, Moftakhari *et al* 2017, Bilskie and Hagen 2018, Gori and Lin 2022), this study demonstrates that current coastal flood hazard assessments can significantly underestimate risk by neglecting rainfall or contributions during extreme coastal events. When rainfall is incorporated into 100 year coastal flood scenarios, compound flooding increased total flooded area by up to 61% compared to coastal-only flooding, with deeply flooded areas (>0.3 m) increased by 4%–30% depending on scenario. While the timing between rainfall and storm surge peaks can influence outcomes, rainfall intensity proved to be the dominant factor in compound flood severity. Urban landforms mediate these effects distinctly: convergent areas experience increased flood depths, while coastal landfills and other urban terrain primarily show expanded flood extent. For areas dominated by flood extent expansion, urban vegetation may offer complementary mitigation potential (Amini *et al* 2025a). Applying the information from historical occurrences of rain and surge helps put these compound scenarios into a useful probabilistic reference frame, with return periods from 160 to 1428 years.

Data availability statement

The data that support the findings of this study will be openly available following an embargo at the following URL/DOI: 10.17632/txy8rdkvf8.1 (Kasaei and Orton 2025).

Supplementary Material available at https://doi.org/10.1088/1748-9326/ae2a55/data1.

Acknowledgments

This research has been supported by the US Geological Survey through the Extending Government Funding and Delivering Emergency Assistance Act (public law 117-43, Award No. G22AC00399-00) under the North Atlantic Coast Co-operative Ecosystems Study Unit (NAC-CESU). We thank Hamed Moftakhari for helpful discussions.

Author contributions

The paper and the experiments were conceptualized by SK, PMO, and JCW. Simulations were done by SK. Statistical analyses were done by SK with help from PMO. The original draft was written by SK with help from PMO; further review was done by PMO, TW, DKR, and JCW; and the edits were done by SK with help from PMO. Project administration was performed by JCW and PMO, and funding acquisition was done by JCW and PMO.

Conflict of interest

The contact author has declared that none of the authors has any competing interests.

ORCID iDs

Shima Kasaei 0000-0003-2331-0100
Thomas Wahl 0000-0003-3643-5463
David K Ralston 0000-0002-0774-3101

References

Abdalla R and Niall K WebGIS-based flood emergency management scenario 2009 *Int. Conf. on Advanced Geographic Information Systems & Web Services* pp 7–12

Ali J, Wahl T, Morim J, Enriquez A, Gall M and Emrich C T 2025 Multivariate compound events drive historical floods and associated losses along the US East and Gulf coasts *npj Nat. Hazards* **2** 19

Amini E, Kasaei S, Marsooli R, Orton P and Hajj M 2025 Assessing future urban flood risks: high-resolution modeling of compound coastal and pluvial flooding *105th Annual AMS Meeting* p 457578

Amini E, Marsooli R and Ayyub B M 2025a Characterizing vegetation effects on wave mitigation performance of resilient hybrid vegetation-seawall systems *Environ. Res. Commun.* **7** 035014

Bates P D, Quinn N, Sampson C, Smith A, Wing O, Sosa J, Savage J, Olcese G, Neal J and Schumann G 2021 Combined modeling of US fluvial, pluvial, and coastal flood hazard under current and future climates *Water Resour. Res.* **57** e2020WR028673

Bilskie M and Hagen S 2018 Defining flood zone transitions in low-gradient coastal regions *Geophys. Res. Lett.* **45** 2761–70

Chen Z, Orton P M, Booth J F, Wahl T, DeGaetano A, Kaatz J and Horton R M 2025 Influence of storm type on compound flood drivers of a mid-latitude coastal urban environment *Hydrol. earth syst. sci.* **29** 3101–17

CIRES: Cooperative Institute for Research in Environmental Sciences (CIRES) at the University of Colorado, Boulder 2014a Continuously updated digital elevation model (CUDEM)—third arc-second resolution bathymetric-topographic tiles [dataset] (available at: https://doi.org/10.25921/ds9v-ky35)

CIRES: Cooperative Institute for Research in Environmental Sciences (CIRES) at the University of Colorado, Boulder 2014b Continuously updated digital elevation model (CUDEM)—1/3 arc-second resolution bathymetric-topographic tiles. [dataset]

Diermanse F, Roscoe K, Van Ormondt M, Leijnse T, Winter G and Athanasiou P 2023 Probabilistic compound flood hazard analysis for coastal risk assessment: a case study in Charleston, South Carolina *Shore Beach* **91** 9–18

EM Center 2017 *North American Mesoscale (NAM) Analysis and Forecast System Characteristics* (Environmental Modeling Center)

FEMA 2014 *Region II Coastal Storm Surge Study: Overview* vol 15 (Federal Emergency Management Agency)

Flood R 2011 *High-Resolution bathymetric and backscatter mapping in Jamaica Bay, Final Report to the National Park Service* (State University of New York at Stony Brook)

Georgas N, Orton P, Blumberg A, Cohen L, Zarrilli D and Yin L 2014 The impact of tidal phase on Hurricane Sandy's flooding around New York City and Long Island Sound *J. Extrem. Events* **1** 1450006

Gori A and Lin N 2022 Projecting compound flood hazard under climate change with physical models and joint probability methods *Earth's Future* **10** e2022EF003097

Hegermiller C A, Warner J C, Olabarrieta M, Sherwood C R and Kalra T S 2022 Modeling of barrier breaching during Hurricanes Sandy and Matthew *J. Geophys. Res.: Earth Surf.* **127** e2021JF006307

Hopper T and Meixler M S 2016 Modeling coastal vulnerability through space and time *PLoS One* **11** e0163495

Jane R, Wahl T, Santos V M, Misra S K and White K D 2022 Assessing the potential for compound storm surge and extreme river discharge events at the catchment scale with statistical models: sensitivity analysis and recommendations for best practice *J. Hydrol. Eng.* **27** 04022001

Jelesnianski C P 1992 *SLOSH: Sea, Lake, and Overland Surges from Hurricanes* (US Department of Commerce, National Oceanic and Atmospheric Administration)

Kasaei S, Orton P M, Ralston D K and Warner J C 2025 Pluvial and potential compound flooding in a coupled coastal modeling framework: New York City during post-tropical Cyclone Ida (2021) *Hydrol. Earth Syst. Sci.* **29** 2043–58

Kasaei S and Orton P 2025 Dataset supporting 'Compounding of 100-year coastal floods by rainfall in an urban environment' *Mendeley Data* **V1**

Kim H, Villarini G, Jane R, Wahl T, Misra S and Michalek A 2023 On the generation of high-resolution probabilistic design events capturing the joint occurrence of rainfall and storm surge in coastal basins *Int. J. Climatol.* **43** 761–71

Kurum O, Kelly D M, Roberts K J and Nairn R2022 *Extreme Rainfall–Runoff Modeling during Remnants of Ida in New York, Coastal Engineering Proc.* p 110

Lewis M, Moftakhari H and Passalacqua P 2024 Challenges for compound coastal flood risk management in a warming climate: a case study of the Gulf Coast of the United States *Front. Water* **6** 1405603

Lin J, Zhang W, Wen Y and Qiu S 2023 Evaluating the association between morphological characteristics of urban land and pluvial floods using machine learning methods *Sustain. Cities Soc.* **99** 104891

Lin N, Emanuel K A, Smith J A and Vanmarcke E 2010 Risk assessment of hurricane storm surge for New York City *J. Geophys. Res. Atmos.* **115**

Lin N, Emanuel K, Oppenheimer M and Vanmarcke E 2012 Physically based assessment of hurricane surge threat under climate change *Nat. Clim. Change* **2** 462–7

Lin N, Kopp R E, Horton B P and Donnelly J P 2016 Hurricane Sandy's flood frequency increasing from year 1800–2100 *Proc. Natl Acad. Sci.* **113** 12071–5

Lopeman M, Deodatis G and Franco G 2015 Extreme storm surge hazard estimation in lower Manhattan: clustered separated peaks-over-threshold simulation (CSPS) method *Nat. Hazards* **78** 355–91

Marsooli R, Lin N, Emanuel K and Feng K 2019 Climate change exacerbates hurricane flood hazards along US Atlantic and Gulf Coasts in spatially varying patterns *Nat. Commun.* **10** 3785

Mattocks C and Forbes C 2008 A real-time, event-triggered storm surge forecasting system for the state of North Carolina *Ocean Modelling* **25** 95–119

Moftakhari H R, Salvadori G, AghaKouchak A, Sanders B F and Matthew R A 2017 Compounding effects of sea level rise and fluvial flooding *Proc. Natl Acad. Sci.* **114** 9785–90

National Oceanic and Atmospheric Administration, O. f. C. M 2016 *Coastal Change Analysis Program (C-CAP) Regional Land Cover [dataset]*

NPCC4 2024 *NPCC4: Climate Change and New York City's Flood Risk* (Wiley) pp 0077–8923

NYC DEP Jamaica Bay Watershed Protection Plan Update, New York City Department of Environmental Protection 2018

NYC 2013 *A Stronger More Resilient New York* pp 107–29

Orton P M, Hall T, Talke S A, Blumberg A F, Georgas N and Vinogradov S 2016 A validated tropical-extratropical flood hazard assessment for New York Harbor *J. Geophys. Res. Oceans* **121** 8904–29

Orton P M, Sanderson E W, Talke S A, Giampieri M and MacManus K 2020 Storm tide amplification and habitat changes due to urbanization of a lagoonal estuary *Nat. Hazards Earth Syst. Sci.* **20** 2415–32

Orton P, Georgas N, Blumberg A and Pullen J 2012 Detailed modeling of recent severe storm tides in estuaries of the New York City region *J. Geophys. Res. Oceans* **117** C09030

Pallathadka A, Sauer J, Chang H and Grimm N B 2022 Urban flood risk and green infrastructure: Who is exposed to risk and who benefits from investment? A case study of three US Cities *Landscape Urban Plann.* **223** 104417

Pawlowicz R, Beardsley B and Lentz S 2002 Classical tidal harmonic analysis including error estimates in MATLAB using T_TIDE *Comput. Geosci.* **28** 929–37

Penny A B, Alaka L, Taylor A A, Booth W, DeMaria M, Fritz C and Rhome J 2023 Operational storm surge forecasting at the National Hurricane Center: the case for probabilistic guidance and the evaluation of improved storm size forecasts used to define the wind forcing *Weather Forecast.* **38** 2461–79

Qi M, Huang H, Liu L and Chen X 2020 Spatial heterogeneity of controlling factors' impact on urban pluvial flooding in Cincinnati, US *Appl. Geogr.* **125** 102362

Rosenzweig B R, McPhillips L, Chang H, Cheng C, Welty C, Matsler M, Iwaniec D and Davidson C I 2018 Pluvial flood risk and opportunities for resilience *Wiley Interdiscip. Rev.* **5** e1302

Rosenzweig B, Montalto F A, Orton P, Kaatz J, Maher N, Kleyman J, Chen Z, Sanderson E, Adhikari N and McPhearson T 2024 *NPCC4: Climate Change and New York City's Flood Risk* (Wiley) pp 0077–8923

Sadegh M, Moftakhari H, Gupta H V, Ragno E, Mazdiyasni O, Sanders B, Matthew R and AghaKouchak A 2018 Multihazard scenarios for analysis of compound extreme events *Geophys. Res. Lett.* **45** 5470–80

Santamaria-Aguilar S, Maduwantha P, Enriquez A R and Wahl T 2025 Large discrepancies between event- and response-based compound flood hazard estimates *EGUsphere preprint* (https://doi.org/10.5194/egusphere-2025-1938)

Santiago-Collazo F L, Bilskie M V and Hagen S C 2019 A comprehensive review of compound inundation models in low-gradient coastal watersheds *Environ. Modelling Softw.* **119** 166–81

Shirzaei M and Bürgmann R 2018 Global climate change and local land subsidence exacerbate inundation risk to the San Francisco Bay Area *Sci. Adv.* **4** eaap9234

Smith H D, Orton P, Sanderson E W and Fischbach J 2018 Integrated modelling to predict landscape evolution, flooding, and water quality in Jamaica Bay, NY *Coast. Eng. Proc.* 13

Svensson C and Jones D A 2004 Dependence between sea surge, river flow and precipitation in south and west Britain *Hydrol. Earth Syst. Sci.* **8** 973–92

Thompson C M and Frazier T G 2014 Deterministic and probabilistic flood modeling for contemporary and future

coastal and inland precipitation inundation *Appl. Geogr.* **50** 1–14

Tonn G and Czajkowski J 2022 Evaluating the risk and complexity of pluvial flood damage in the US *Water Econ. Policy* **8** 2240002

Wang H V, Loftis J D, Liu Z, Forrest D and Zhang J 2014 The storm surge and sub-grid inundation modeling in New York City during Hurricane Sandy *J. Mar. Sci. Eng.* **2** 226–46

Wang Z, Leung M, Mukhopadhyay S, Sunkara S V, Steinschneider S, Herman J, Abellera M, Kucharski J, Nederhoff K and Ruggiero P 2024 A hybrid statistical–dynamical framework for compound coastal flooding analysis *Environ. Res. Lett.* **20** 014005

Wang Z, Leung M, Mukhopadhyay S, Sunkara S V, Steinschneider S, Herman J, Abellera M, Kucharski J and Ruggiero P 2025 Compound coastal flooding in San Francisco Bay under climate change *npj Nat. Hazards* **2** 3

Warner J C, Armstrong B, He R and Zambon J B 2010 Development of a coupled ocean–atmosphere–wave–sediment transport (COAWST) modeling system *Ocean Modelling* **35** 230–44

Warner J C, Defne Z, Haas K and Arango H G 2013 A wetting and drying scheme for ROMS *Comput. Geosci.* **58** 54–61

Xu H, Xu K, Bin L, Lian J and Ma C 2018 Joint risk of rainfall and storm surges during typhoons in a coastal city of Haidian Island, China *Int. J. Environ. Res. Public Health* **15** 1377

Zachry B C, Booth W J, Rhome J R and Sharon T M 2015 A national view of storm surge risk and inundation *Weather Clim. Soc.* **7** 109–17

Zellou B and Rahali H 2019 Assessment of the joint impact of extreme rainfall and storm surge on the risk of flooding in a coastal area *J. Hydrol.* **569** 647–65

Zhang F and Orton P M 2022 Importance of neighborhood aspect ratio and storm climate to adaptation efforts to reduce coastal flood mortality *Front. Built Environ.* **7** 769161